Journal of Polymers and the Environment (2020) 28:500–516
https://doi.org/10.1007/s10924-019-01622-9

ORIGINAL PAPER

Green Microcomposites from Renewable Resources: Effect of Seaweed (*Undaria pinnatifida*) as Filler on Corn Starch–Chitosan Film Properties

Danila Merino[1,2] · **Vera A. Alvarez**[1]

Published online: 2 December 2019

Abstract

Natural seaweed microparticles obtained from *Undaria pinnatifida* waste (A) were used as fillers in thermoplastic starch (TPS)–chitosan (CH) blend in order to obtain microcomposites films for application in sustainable agriculture. The adequate proportion of both polymers was optimized with regards their mechanical, barrier, water interaction and morphological properties. Then, the effect of different content of seaweed on microcomposites properties was investigated. The seaweed used showed good interaction with the TPS–CH matrix. Its addition produced an increase in the tensile strength and a slight increase in the elongation at break. Contents of 10% of A lead to a more heterogeneous structure with the formation of aggregates. Low contents of A reduced the mobility of the polymer chains resulting in a lower moisture content and higher T_g, although the WVP increased with the content of A. The improvements achieved with microcomposites were finally discussed under the light of new agricultural mulch films regulations.

Keywords Sustainable · Algae · Bio-based · Composite · Blend

Introduction

The use of plastic mulches in various agricultural crops has been shown to have an impact on the increase of their yields and to produce less dependence on herbicides and pesticides, as well as to contribute to a better efficiency in the use of water, which is a promising alternative for intensive crops in poor soils or with low humidity and organic matter [1]. Agricultural mulches are commonly used for the intensive cultivation of fruits and vegetables and are the most economically convenient option for farmers [2]. In general, horticultural production without coverage is limited for climatic reasons to the warmer months of the year. The species that have high temperature requirements need to be grown in greenhouses, even in the warmer spring–summer season. Given that the construction of greenhouses has a high cost, and producers must ensure that the crops are economically profitable and biologically viable, the use of mulches usually results in a possible alternative to achieve both objectives [3].

At present, the polymer that is mostly used in the formulation of mulches is polyethylene (PE), which is a non-biodegradable material derived from petroleum. Therefore, once the crop cycle has ended, it must be manually removed, a task that is laborious, economically unfavorable and often not performed [4].

This work proposes to develop and study the properties of a biodegradable polymeric material based on starch and CH for the potential manufacture of biodegradable agricultural mulches. The films will be prepared by casting, a technique that allow obtaining TPS when heating starch in presence of water and a plasticizer [5]. Starch is a widely available natural and economic polymer synthesized by plants. This polymer, despite to be widely available and economic, has some disadvantages such as high hydrophilicity and poor mechanical properties associated with their

Electronic supplementary material The online version of this article (https://doi.org/10.1007/s10924-019-01622-9) contains supplementary material, which is available to authorized users.

✉ Danila Merino
danila.merino@fi.mdp.edu.ar

[1] Grupo de Materiales Compuestos Termoplásticos (CoMP), Instituto de Investigaciones en Ciencia y Tecnología de Materiales (INTEMA), Facultad de Ingeniería, Universidad Nacional de Mar del Plata (UNMdP) y Consejo Nacional de Investigaciones Científicas y Técnicas (CONICET), Av. Colón 10850, 7600 Mar del Plata, Argentina

[2] Present Address: Smart Materials Group, Italian Institute of Technology (IIT), Via Morego 30, 16163 Genoa, Italy

brittleness [6]. A strategy commonly used to improve the properties of starch is the formation of mixtures or blends with other polymers [7, 8]. For example, previous studies have reported that mixing TPS with CH produces improvements in the mechanical properties of starch films, while providing antibacterial activity [9].

CH is a linear polysaccharide constituted to a greater extent of units of β-1,4-D-glucosamine and to a lesser extent of N-acetyl-D-glucosamine. It is obtained from chitin, which is obtained mainly from residues from marine foods such as shells of crabs and prawns. Its annual production exceeds 10×10^{11} tons, of which 2000 tons of CH are obtained annually, with chitin being the second most abundant renewable polymer in the world [10]. Additionally, it has been reported in the literature that this polymer has important applications in agriculture. It acts as an inducer of the defense response against biotic stress in plants [11–13] and has antimicrobial [14–16] and biostimulant properties [17–19].

The mentioned materials were used in the formulation of microcomposites with a bioactive material such as the microparticles of the seaweed *Undaria pinnatifida* (A), which is expected to add value to the biodegradable thermoplastic film by generating new functionalities. *Undaria pinnatifida* is a species of seaweed with important properties in agriculture, among which its ability to induce the defense response in plants and stimulate its growth stand out [20, 21].

Seaweed represents a wide and economical source of potential fillers for the preparation of polymeric compounds, however, the work that can be found in literature to know the properties of this type of materials is very scarce [22, 23]. Some authors have used them for the preparation of microcomposites films with polylactic acid (PLA) [22], polyvinyl alcohol (PVA) [23], soy protein [24], polybutylene adipate terephthalate (PBAT) [25] and with the starch-agar blend [26].

In this work we report the synthesis and characterization of corn starch-chitosan microcomposites obtained with seaweed microparticles. Initially, the selection of the appropriate TPS/CH ratio was made for the formulation of microcomposite thermoplastic films with A. Then, the effect of different contents of A on the properties of these films was reported and analyzed and their potential application as agricultural mulches was discussed.

It is hypothesized that the mixture of starch with CH can produce improvements on the mechanical properties of the starch, that the addition of algae can have positive impacts in terms of mechanical and barrier properties of microcomposites and that these can contribute to increase the opacity and to reduce the transmissivity coefficient of photosynthetically active radiation (PAR).

Materials and Methods

Materials

Corn starch and glycerol were purchased from Dos Hermanos distribuidora (Mar del Plata, Argentina) and Química DEM (Mar del Plata, Argentina), respectively. Corn starch characterization yielded a molecular weight higher than 2000 kDa determined by gel permeation chromatography (GPC) in a high resolution liquid chromatography system (GPC-HPLC). In addition, a percentage of 19% of amylose content was determined by using the method reported by Stawski [27]. CH and acetic acid (HAc) were from Drogueria Saporiti (Buenos Aires, Argentina) and BioPack (Buenos Aires, Argentina), respectively. CH characterization indicated a molecular weight of 535 kDa determined using the method reported by De la paz et al. [28] and a deacetylation degree higher than 90% obtained by NMR [29]. Seaweed microparticles were obtained from Soriano S.A. (Chubut, Argentina). The cell wall of these algae is composed mainly of the polysaccharides fucoidane, sodium alginate, laminarin and its derivatives and represent between 10 and 20% (w/w). The protein content is generally between 6 and 13% (w/w), while the lipid content is relatively lower, between 0.57 and 3.5% (w/w) [30]. Britt and Kangas [31] have reported a mineral content of between 60 and 80% dry weight of these algae. The characterization of the mineralogical composition of the alga used indicates a high prevalence of potassium, phosphorus, sodium, calcium and magnesium with a lesser content of iron, copper, zinc and iodine. The particle size of the alga was determined using a series of sieves (Zonytest, Buenos Aires, Argentina) with meshes of 500, 250, 105 and 74 µm. The results indicated that the 79% of them were in the range of 74 and 250 µm, 18% under 74 µm and the rest in between 250 and 500 µm.

Blends Preparation and Selection of TPS/CH Ratio

CH solution (1% w/v) was prepared in HAc (1% v/v) by stirring at 60 °C until complete dissolution. Simultaneously, a corn starch solution (1% w/v) was prepared in distilled water together with glycerol as plasticizer (30% w/w). To assure starch complete gelatinization, the mixture was heated at 90 °C and homogenized with a digital Ultra Turrax (IKA, model T25) at 10,000 rpm during 30 min. Once both solutions were prepared they were mixed at adequate proportions in order to obtain 100% thermoplastic chitosan (CH), 25% thermoplastic starch (75%CH), 50% thermoplastic starch (50%CH), 75% thermoplastic starch (25%CH) and 100% thermoplastic starch

(TPS). The homogenization was prolonged 15 min more and the final blends were placed in a refrigerator overnight in order to eliminate air bubbles. Then, the film-forming solutions were poured into Teflon-covered plates and dried in an oven at 45 °C during 48 h. Films were finally peeled off and conditioned as reported below.

Films were characterized in order to select the appropriate formulation for the preparation of microcomposites. For that mechanical, water barrier, water interaction and morphological properties were evaluated as described below.

Microcomposites Preparation

The microcomposite materials were obtained by incorporating A in 0.5, 1, 2 and 10% (w/w) to the formulation of the film with the best properties, 75CH. The procedure used was similar to the one reported in "Blends preparation and selection of TPS/CH ratio" section. A 1% (w/v) CH solution in 1% HAc (v/v) was prepared and mixed with a 1% (w/v) corn starch solution together with 30% (w/w) of glycerol. The mixture was maintained at 10,000 rpm with a homogenizer for 30 min. Next, A was added and homogenization was maintained for an additional 30 min. These materials were designated 75CH + 0.5A, 75CH + 1A, 75CH + 2A and 75CH + 10A.

Conditioning

All samples were conditioned during 1 week before characterization. For that, films were stored in a chamber at constant relative humidity of 60% and temperature of 20 °C ± 2 °C. Chamber relative humidity was achieved with a solution of water–glycerin.

Characterization

Film Thickness

The films thickness was measured at five points with a digital micrometer (Rokoo, 0–25 mm, 0.001 mm resolution) and averaged to be used in WVP and tensile tests.

Scanning Electron Microscopy (SEM)

The microstructural analysis of the cross-section of blends and microcomposites was carried out in a Field emission scanning electron microscope (FE-SEM) Ultra 55, Zeiss. Film samples were prepared by cryofracture by submerging in liquid air. Then, they were fixed to glass stubs with silicon and finally covered with a thin layer of gold.

Fourier Transform Infrared Spectroscopy (FTIR)

FTIR of films were measured using an attenuated refraction (ATR) accessory in an IR spectrometer (PerkinElmer spectrum 100). The films were grid onto the diamond surface of the ATR accessory and the spectra were recorded in the range of 4000 to 600 cm^{-1} at a 4 cm^{-1} resolution and 32 consecutive scans were averaged.

Thermogravimetric Analysis (TGA)

A Thermogravimetric analyzer (TA Q500 HI-Res™) was used in order to determine the thermal stability and temperatures of thermal degradation events under air flow (50 ml/min). Samples were heated from 30 to 900 °C at 10 °C/min. Nearly 20 mg of each sample was used in each test. Initial and final temperatures and the maximum of each event together with the mass loss were obtained from the first derivative of the residual mass (%) vs. temperature (°C) curves (DTGA curves).

Differential Scanning Calorimetry (DSC)

DSC analysis was performed in a TA Q2000 differential scanning calorimeter with a cooling system under nitrogen flow (50 ml/min). All samples were in the range of 3–6 mg and once weighted they were placed in aluminum pans and sealed. The applied cycle consisted in heating samples from − 90 to 200 °C at a heating rate of 10 °C/min. Curves obtained were utilized for glass transition temperature (T_g) determination.

Moisture Content (MC)

The moisture content of the films was determined gravimetrically after each sample was dried at 100 °C for 24 h. The MC (%) was then calculated by using the following Eq. (1):

$$MC(\%) = \frac{m_i - m_f}{m_i} x100\% \quad (1)$$

where m_i and m_f are the initial and final mass of each sample respectively. The assay was performed in triplicate and the results were informed as average ± standard deviation (SD).

Water Solubility (WS)

The films water solubility was evaluated by submerging approximately 0.5 g of previously dried at 100 °C during 24 h sample into 30 ml of distilled water. The recipients were kept overnight and then the films were recovered

and dried again at 100 °C during 24 h for measuring their final mass. Water solubility was calculated following the equation (2):

$$WS(\%) = \frac{(m_i - m_f)}{m_i} \times 100\% \quad (2)$$

where m_i and m_f are the initial and final mass of the film respectively.

Moisture Absorption at Equilibrium (MA_{eq})

Samples of 1 cm^2 were cut out and dried in an oven at 40 °C for 48 h. Then, their initial weight was recorded and placed in controlled humidity containers. The moisture absorption of the films was studied at room temperature (20 °C) and 90% RH. The mass of each sample was recorded regularly for 2 weeks. The moisture absorption (MA) was determined using Eq. (3):

$$MA(\%) = \frac{m_t - m_0}{m_0} \times 100\% \quad (3)$$

where m_t is the mass of the sample at time of exposure t and m_0 is the initial mass of the dry sample. The results were expressed as the AH_{eq} (%) ± SD, being AH_{eq} (%), the registered moisture absorption once equilibrium was reached. The tests were carried out in triplicate.

Water Vapor Permeability (WVP)

The water vapor permeability assay was performed as indicated in the standard ASTM E96-00e1 [32]. Previously dried calcium chloride was placed in the permeability cups (4.9 cm diameter and 1.8×10^{-3} m^2 exposed area) in order to make a 0% RH inside the capsule. Sealed capsules with the films tested were weighted and then placed in a chamber at constant 60% relative humidity and 20 °C. The capsules were weighted every hour during the first 8 h using an analytical balance and then once per day. To calculate the water vapor transmission rate (WVTR) a plot of weight gained (g) as function of time (h) was performed. Their slope in the steady state was taken as WVTR and used in the following equation (4) in order to obtain de WVP:

$$WVP = \frac{WVTR \times l}{A \times \Delta P} \quad (4)$$

where l is the average thickness of each film in m, A is the exposed area in m^2 and ΔP is the pressure difference between the one bellow the film and that of above it in Pa. Each sample was analyzed by triplicate and the results are expressed as mean ± SD.

Mechanical Properties

Mechanical properties by means of tensile tests were measured in a universal test machine INSTRON EMIC23-50 as indicated in ASTM D882-02 standard. The crosshead speed was set at 2.5 mm/min, the load cell was 50 N and the distance between film-grips was 3.5 cm. Stress–strain curves were obtained and from there, the elastic modulus (E), the maximum tensile strength (σ_m) and the elongation at break (ε_b) were calculated. Ten replicates were analyzed by sample at room temperature and the results were expressed as mean ± SD.

Transparency (T)

The transmittance of the films developed was measured using an Agilent 8453 spectrophotometer in the wavelength range from 290 to 1100 nm. For this, the samples were cut into rectangular pieces of 4 cm × 2 cm, their thickness was measured in five points and they were stuck to the measuring cell with adhesive tape. Once the spectra were obtained, the transparency was calculated using Eq. (5) [33].

$$T = \frac{-\log T_{600}}{l} \quad (5)$$

where T is the transparency, T_{600} is the transmittance at 600 nm and l is the average thickness of the film in mm.

Radiometric Properties

The direct transmissivity in the PAR range (τ_{PAR}) was measured using an Agilent 8453 spectrophotometer. The coefficients were obtained using the following equation (6):

$$\tau_{PAR} = \frac{\sum_{\lambda=400nm}^{\lambda=700nm} S_\lambda \Delta\lambda \tau(\lambda)}{\sum_{\lambda=400nm}^{\lambda=700nm} S_\lambda \Delta\lambda} \quad (6)$$

where S_λ is the spectral distribution of the sun at the wavelength λ [34], Δλ, is the wavelength range equal to 50 nm and τ (λ), is the spectral transmittance at the wavelength λ.

Statistical Analysis

The statistical analysis of experimental results was performed through one-way analysis of variance (ANOVA) using Tukey's multiple comparison test with a 95% level of confidence ($p < 0.05$) in order to analyze significant differences.

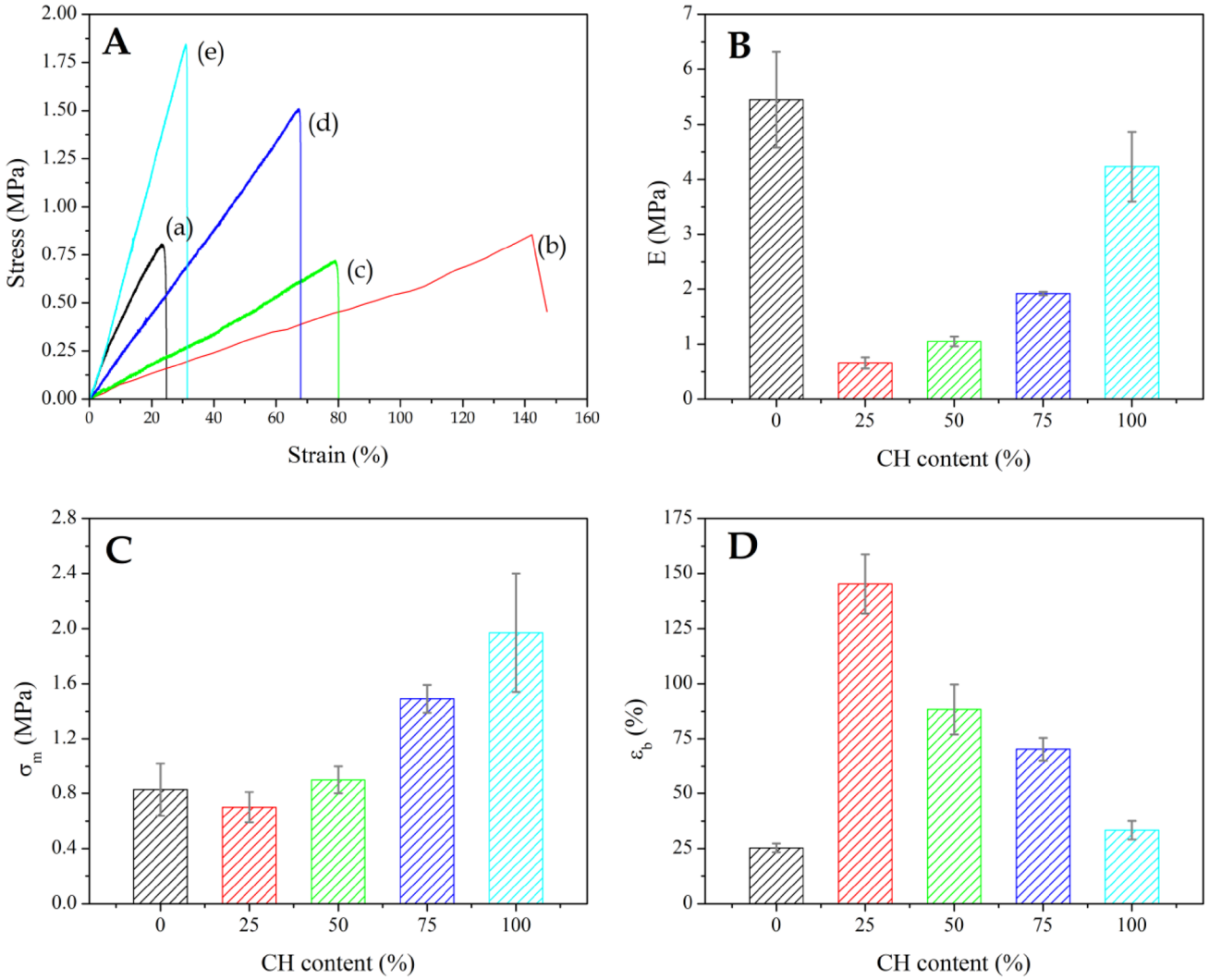

Fig. 1 Mechanical properties of TPS/CH blends. **A** Stress (MPa) vs. strain (%) curves for *a* TPS, *b* 25CH, *c* 50CH, *d* 75CH and *e* CH; **B** E (MPa); **C** σ_m (MPa) and **D** ε_b (%) as a function of CH content (%)

Results

Selection of the Appropriate TPS/CH Ratio for the Preparation of Microcomposites

Figure 1 presents the results of the mechanical properties of the materials studied.

Clearly, the incorporation of CH to the starch matrix in a percentage of 25% produced a plasticizing effect. There was a marked decrease in the E and an increase in the ε_b with the addition of CH in the mixture. These results are in accordance with those described by Luchese et al. [35] and Pelissari et al. [36] who observed the plasticizing effect by incorporating 14% (w/w) and 5% (w/w) CH to starch, respectively. Such behavior can be attributed to the fact that hydrogen bond interactions between starch molecules are interrupted by the presence of CH molecules. Therefore, the decrease between the intermolecular starch forces would produce a decrease in the σ_m of the material [37, 38]. A plasticizer reduces intermolecular forces and increases the separation between molecules making the structure less dense [39].

On the other hand, increases in the CH content produced an increase on the E and the σ_m of the material and a consequent decrease in the ε_b. This behavior was previously observed by other authors [40–42]. Bourtoom and Chinnan [40] explained that increasing the percentage of CH in the mixture increases the number of NH_3^+ groups and therefore new hydrogen bonding interactions are generated between the hydroxyl groups of the starch resulting in a more rigid polymer network [40]. Thus, CH acts as a reinforcing agent in the structure of starch [41].

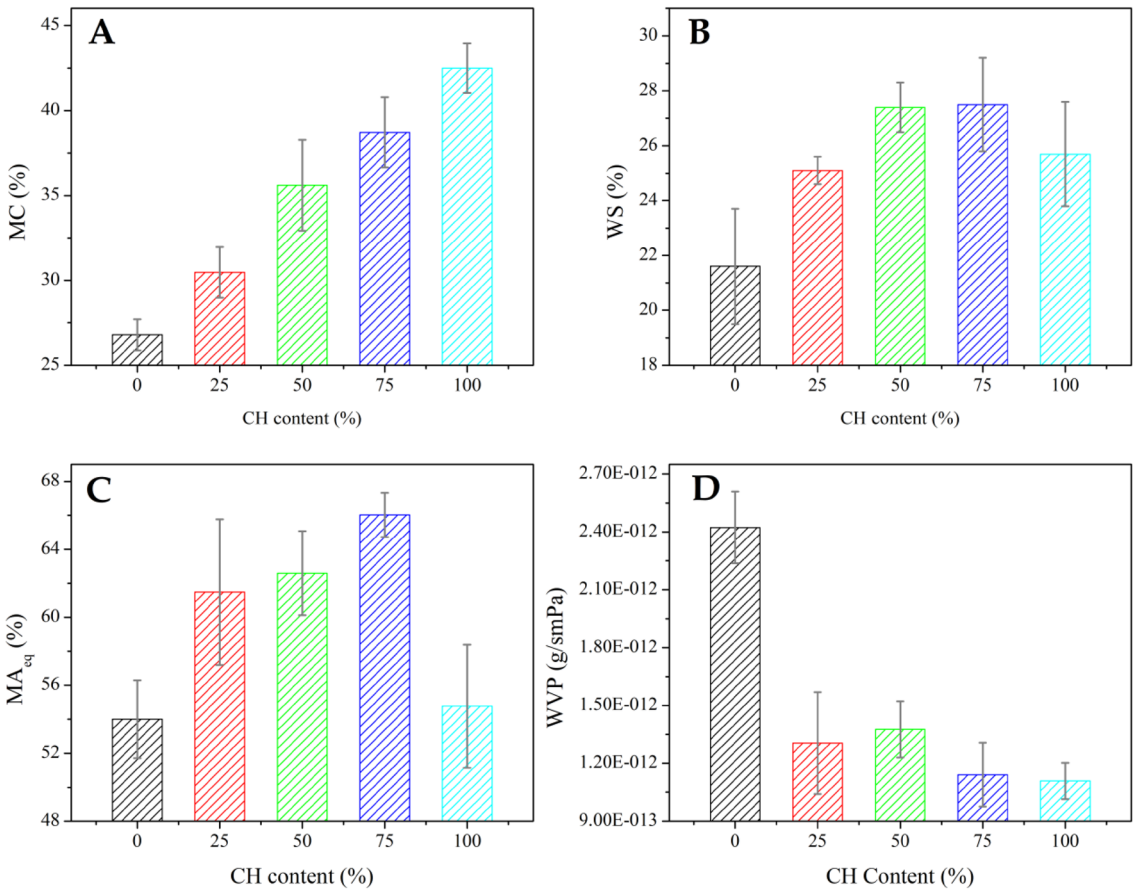

Fig. 2 Interaction of materials with water as a function of the CH content (%) in the blend. **a** MC (%); **b** WS (%); **c** MA_{eq} (%) in atmosphere at 90% RH and; **d** WVP (g/s m Pa)

In our work, no significant differences in the σ_m of the samples with 0, 25 and 50% of CH were observed being the increase on the strength significant in the sample 75CH.

Regarding the interaction of the developed materials with the water, it was found that the MC (Fig. 2) increased with the CH content. This behavior has been previously explained by other authors who argue that CH being more hydrophilic than starch, by the presence of NH_3^+ groups, tends to retain more water molecules in its structure [38, 40].

In general, no significant differences were found ($p < 0.05$) in WS (Fig. 2B) for blends and in all cases their value was less than 30%. The material dissolved in water was most likely the plasticizer glycerol [37, 39]. Additionally, no ruptures or fragmentations were observed after the test, so that the polymer network seems to remain intact and only low molecular weight substances could have been released [40]. The results obtained were similar to those reported by Bourtoom [37] for mixtures of TPS/CH 1:1 and glycerol contents between 20 and 60% (w/w).

Regarding the MA_{eq} (Fig. 2C), both the TPS and the CH showed no significant differences while the mixtures showed slightly higher values (greater than 60%), which could be related to the greater availability of protonated amino groups and the presence of a more open structure and with greater availability of polar groups to interact with water molecules. It was experimentally observed that the films exhibiting low CH contents arched in the environment in which the experiment was carried out. This can be explained by considering that the network of the CH polymer is more rigid than that of TPS since the latter is more flexible because of the presence of branched molecules of amylopectin, which results in a structure less dense than that of the CH, constituted by polycationic and linear molecules [42]. It was also observed that the starch films were completely colorless, while those of CH were light yellow; and that as the CH content in the starch mixtures increased, the films became more yellowish. This coloration can be attributed to the formation of products of the Maillard reaction, commonly referred to the reaction between sugars and proteins, in this case, comprising the amino groups of the CH polymer [42].

The WVP of the mixtures was evaluated at a vapor pressure difference across the film of 0/60% RH. Figure 2D shows that the WVP decreased with the increase in the CH content in the mixture. This tendency can be explained

by considering the changes suffered by the network of the base polymer when adding another substance in its structure [37]. The improvement in the barrier properties of starch, by incorporating CH molecules in its structure can be also attributed to the increase in the interactions between these two polymers [38]. The values obtained were between 1.2 and 2.5 × 10^{-12} g/s m Pa and were much lower than those reported by Ren et al. [38] between 1.2 and 3 × 10^{-10} g/s m Pa for TPS/CH mixtures with up to 80% of the latter (test carried out with a humidity gradient of 0/95% RH) and by Zhong et al. [43] for 50% TPS/CH mixtures with values of 4–5 × 10^{-10} g/s m Pa (test carried out with a humidity gradient of 0/75% RH). However, they are similar to those obtained by Dang and Yoksan [44] for starch films with CH contents of less than 2% (between 3 and 4 × 10^{-12} g/s m Pa), measured with a humidity gradient of 0/50% RH. These authors explain that these effects may be due to the presence of acetyl groups in the CH or to the hydrogen bridge interaction between their polymer chains and those of the TPS that could reduce the number of free OH^- to interact with the water molecules.

Figure 3 shows the micrographs of the SEM cryofracture zone obtained in the FE-SEM.

It was observed that TPS presented a fracture surface with microcracks or cracks, which is directly related to the intrinsic fragility of this material [45] and justifies its initial behavior in the test of mechanical properties (Fig. 1). CH presented a surface with striations. The mixtures with CH presented in all cases a smooth and homogeneous surface. The presence of different phases or granules of starch was not observed. Therefore, it is considered that gelatinization was complete [45] and that both polymers (starch and CH) are highly compatible [9]. Similar results, regarding the appearance of the samples and compatibility between the polymers, were previously described by Bonilla et al. [9], Ren et al. [38] and Lozano-Navarro et al. [46].

Based on the observations mentioned above, the sample 75CH was selected as a matrix for the preparation of microcomposites with A. In particular, 75CH showed

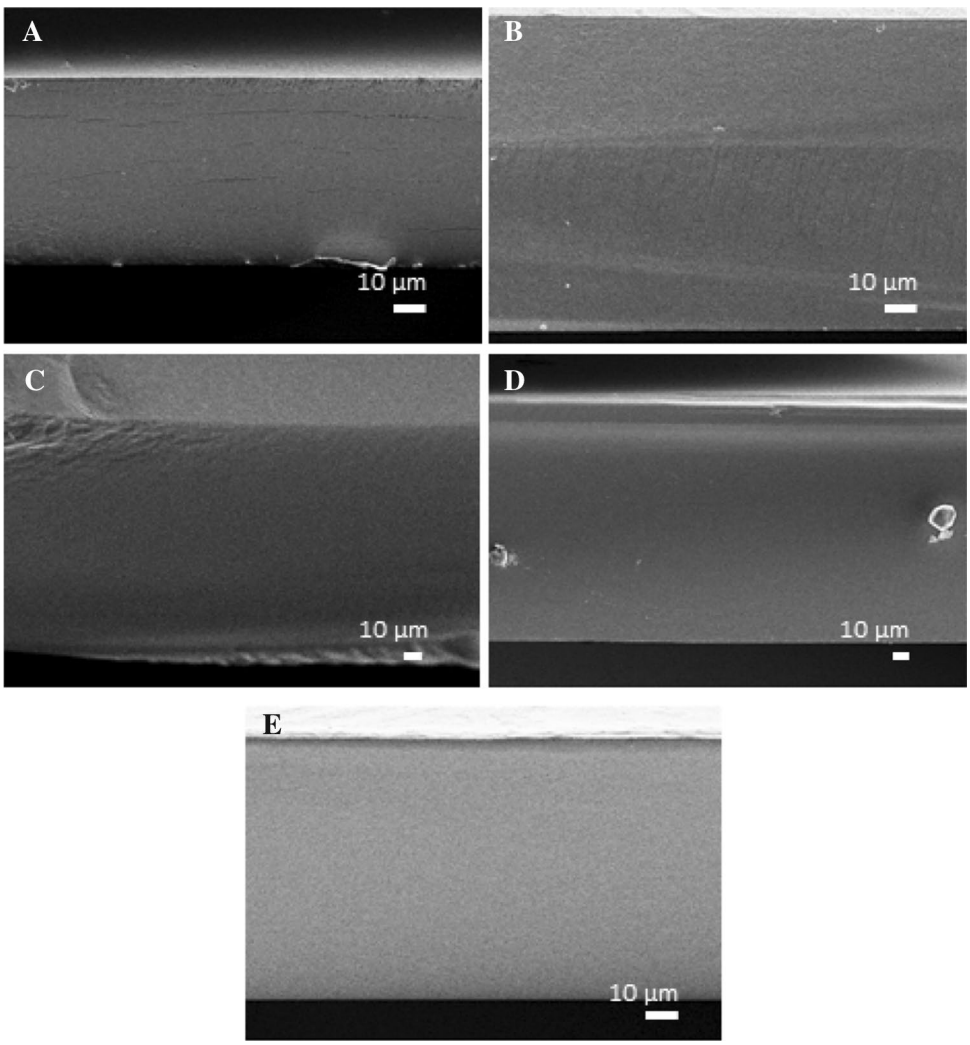

Fig. 3 SEM micrographs for **a** TPS, **b** CH, **c** 25CH, **d** 50CH and **e** 75CH

improvements in σ_m with respect to pure starch and a reasonable value of ε_b (60%) (Fig. 1). Regarding its relationship with water, it exhibited a high MA_{eq} and MC, although in general the difference with the other mixtures was very small (Fig. 2). However, it should be noted that it maintained its shape in environments conditioned at 90% RH and showed very good barrier properties against water vapor (Fig. 2).

Effect of the Incorporation of A Microparticles

Once the microcomposites were obtained, they were analyzed by using FTIR in order to study the chemical interactions between the constituent polymers of the mixture and the natural filler added in different proportions. Figure 4A presents the infrared absorption spectra of (a) TPS, (b) CH and (c) 75CH.

Both the CH and the TPS presented the typical bands associated with the presence of their O–H groups: 3295 cm^{-1} for starch and 3245 cm^{-1} for O–H together with N–H for CH [38]. The starch presented a stretching band at 1650 cm^{-1} due to the presence of water adsorbed and the CH presented two bands, at 1547 and 1640 cm^{-1}, associated with the bending of the N–H (amide II) bond and the stretching of C=O (amide I), respectively [38, 40]. The stretching band at 1152 cm^{-1} for TPS is associated with the C–O stretch in C–O–H and the band at 1002 cm^{-1} is attributed to the stretching of C–O in C–O–C [38] while for CH, similar bands were observed showing the structural similarity that present both polysaccharides.

The 75CH mixture had mainly the same bands as the CH and shifts were observed at the position of several absorption bands, which indicates that there was interaction with the starch [38]. Particularly, the absorption band due to the O–H stretching appears at 3276 cm^{-1} for the 75CH sample, adopting an intermediate value to that presented by the TPS and the CH. Additionally, the band that appears at 1547 cm^{-1} in CH runs at 1554 cm^{-1} for 75CH, indicating the presence of hydrogen bond interactions between the hydroxyl groups of the starch and the protonated amino of the CH. Bourtoom and Chinnan [40] and Ren et al. [38] have found similar results that are in agreement with those obtained in the WVP, SEM and mechanical properties presented above.

Figure 4B shows infrared absorption spectra for microcomposites with A. Curve (a) corresponds to the absorption spectrum of the alga used as filler. According to Gomez-Ordoñez and Rúperez [47], brown algae are constituted mainly of sodium alginate (Alg) polysaccharide, since it is part of the cell wall and the intercellular spaces in some of these species of brown seaweed. In this way, it is expected that the main bands of this polymer appear in the infrared spectrum. Absorption bands were found at 3259 and 3197 cm^{-1}, attributed to the stretching vibration

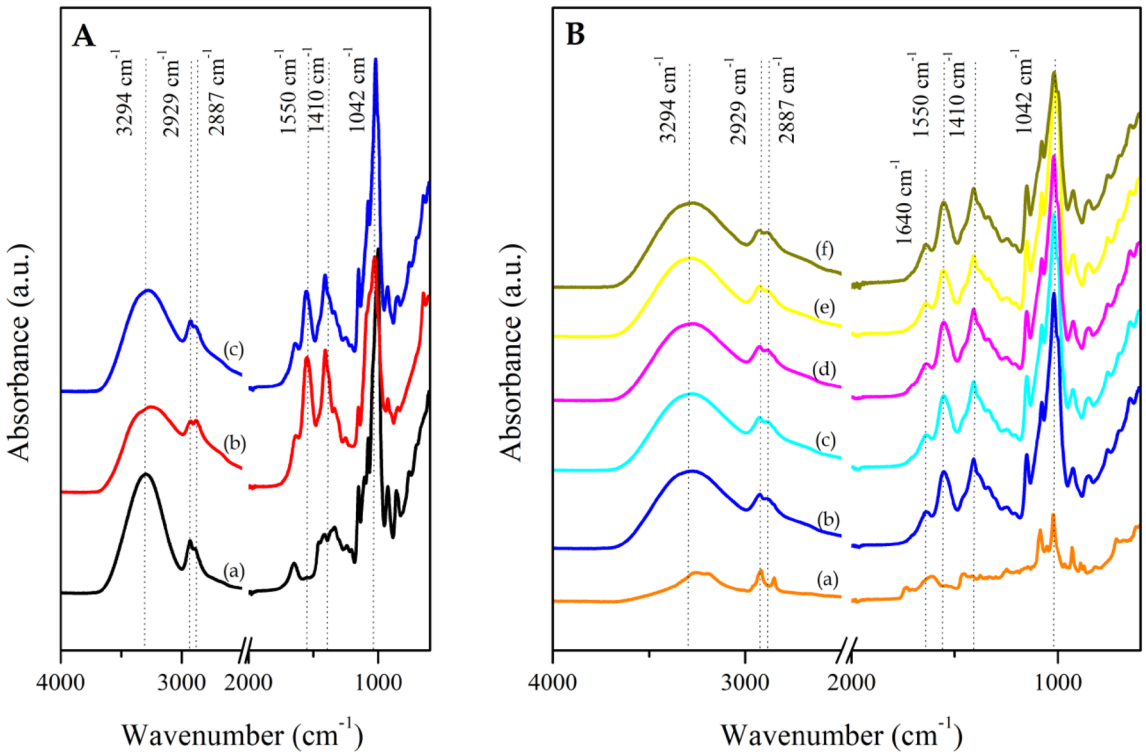

Fig. 4 FTIR of **A** *a* TPS, *b* CH and *c* 75CH. **B** *a* A, *b* 75CH, *c* 75CH + 0.5A, *d* 75CH + 1.0A, *e* 75CH + 2A and *f* 75CH + 10A

of the O–H group present in polysaccharides and N–H of their proteins, bands at 2917 and 2848 cm^{-1}, related to the stretching of C–H groups, 1730 and 1610 cm^{-1}, related to the frequency of stretching of C=O in COOH and COO^{-}, respectively, which indicates the presence of alginic acid and Alg in the structure according to that reported by Gómez-Ordoñez and Rúperez [47]; 1455 cm^{-1}, to the deformation C–O in C–O–H with contribution of the symmetric stretching band of O–C–O of the carboxylate group. The bands at 1083 and 1022 cm^{-1} are attributed to the stretching vibrations of C–O and C–C of the pyranose ring. Finally, in the 950–750 cm^{-1} region are the three main bands of absorption of Alg: 930 cm^{-1}, associated with the stretching of C–O guluronic residues; 874 cm^{-1}, to the deformation C1–H of the mannuronic residues and; at 817 cm^{-1}, characteristic of the manuronic groups [47]. In this way, Alg is the main polysaccharide found in the seaweed studied, despite the small band at 1730 cm^{-1} of the alginic acid found in a lesser proportion. This alga also presented a band at 1246 cm^{-1} commonly attributed to the presence of sulphate groups (S=O) characteristic of other sulfated polysaccharides also present in them [47].

The following curves (c–f) show the absorption spectra of microcomposites with different contents of A. It was found that the addition of A did not considerably affect the infrared absorption spectra and given that the alga is constituted mainly by the Alg polymer, its main absorption bands appear in the absorption zone of other polysaccharides, such as starch and CH and therefore its presence could not be observed [47]. Additionally, there were no changes in the position of the bands, perhaps due to the low percentages of alga used. Similar results were reported by Jumaidin et al. [26], for starch/agar microcomposites with the red algae *Eucheuma cottonii*, who observed shifts in the O–H bands only for A contents greater than 10%.

The effect of different contents of A on the thermal stability of the 75CH matrix was studied by TGA (Curves are included as supplementary material). Table 1 summarizes

Table 1 Main thermal degradation temperatures and associated mass losses for TPS, CH, 75CH and their microcomposites with A

Muestra	T_{inicio} [±0.1] (°C)	T_{fin} [±0.1] (°C)	T_{max} [±0.1] (°C)	Δm [±0.02] (%)	T_{g1} (°C)	T_{g2} (°C)	τ_{PAR} (%)
TPS	30.0	95.0	52.0	4.4	− 78.4	–	
	95.0	230.0	158.6	21.5			
	230.0	395.2	314.2	51.5			
	395.2	543.9	478.3	22.1			
CH	30.0	105.3	78.5	8.2	− 49.9	57.3	
	105.3	232.2	166.6	26.9			
	232.2	418.9	274.4	32.0			
	418.9	643.1	602.1	32.2			
75CH	30.0	101.5	72.4	7.3	− 54.3	49.2	38.3
	101.5	227.3	156.5	25.5			
	227.3	414.8	275.4	35.6			
	414.8	620.6	568.5	31.1			
75CH + 0.5A	30.0	109.3	78.6	7.4	− 63.5	–	30.6
	109.3	228.2	178.0	23.9			
	228.2	410.6	275.3	36.2			
	410.6	664.7	545.8	30.6			
75CH + 1A	30.0	134.0	105.3	10.4	− 68.2	–	29.7
	134.0	240.5	199.5	21.3			
	240.5	414.8	289.8	37.2			
	414.8	785.7	547.0	29.7			
75CH + 2A	30.0	136.1	107.2	9.4	− 55.4	53.3	29.9
	136.1	238.4	193.4	18.7			
	238.4	415.9	281.5	40.3			
	415.8	773.4	558.1	30.9			
75CH + 10A	30	115.5	90.9	8.9	− 60.6	50.1	3.7
	115.5	233.4	183.2	25.5			
	233.4	410.6	281.5	34.5			
	410.6	639.0	542.7	15.9			
	639.0	816.0	787.8	14.1			

the main mass and temperature losses of each degradation event.

The obtained information suggests that all samples have four stages of mass loss, the first two being lower than 200 °C attributed to the loss of weakly absorbed water and structural water together with other volatile compounds such as residues of acetic acid and glycerol (boiling temperature approximately 182 °C), respectively [24, 26, 45]. The temperatures at which both degradation events occur were greater for CH than for TPS, suggesting that CH retains the water and glycerol molecules more strongly than TPS. The same has been observed previously by Merino et al. [48] and was previously mentioned when analyzing the behavior of the different TPS/CH mixtures in a humid environment. In fact, as explained by Debandi et al. [49], CH produces films where their linear molecules are oriented in layers and when there is the presence of glycerol, it is arranged between the polymer chains, increasing their separation and interacting strongly with hydrogen bonds with their amino groups. Then, the plasticizer molecules are grouped together by the formation of hydrogen bonds, thus favoring the absorption of water molecules [49].

The third event is attributable to the thermal and oxidative degradation of the polymers present in each sample [46]. Regarding the degradation temperatures, it was observed that TPS presented a greater thermal stability (314 °C) than CH (274.4 °C) and 75CH (275.4 °C). These values are similar to those previously reported by other authors [9, 45].

Regarding the 75CH blend, an intermediate thermal stability between that of CH and that of TPS would be suggesting a good compatibility between the involved polymers given the presence of strong intermolecular interactions, as indicated by the analysis of the infrared spectra and has been previously suggested by Mathew et al. [42].

Finally, the TPS sample presented a last peak of degradation associated with the oxidative degradation of the carbonaceous residue of the previous step at 478.3 °C and with a mass loss of 22.1%, whereas CH presented this stage at a higher temperature and with a mass loss superior (602.1 °C and 32.2%) [50, 51]. The mixture 75CH, on the other hand, showed again an intermediate behavior closer to that of the CH.

The thermogravimetric analysis of A presented peaks of degradation with maximums at 47, 250, 278, 346, 770 and 876 °C. As reported by Bulota and Budtova [22], the first mass loss occurs for all algae at around 60 °C and is associated with the degradation of chlorophyll together with the evaporation of water [22]. The following degradation temperatures are attributed to the degradation of polysaccharides and other biomolecules: proteins, lipids, phenolic compounds and terpenoids, among others [30, 52], while the events that occur at higher temperatures are attributed to the presence of inorganic matter due to the high contents of salts and impurities that the algal biomass possesses [22].

With regard to the microcomposites, again at least four events of mass loss were found, with curves very similar to that of the 75CH blend. The first two events are attributed to the loss of water slightly adsorbed (below 100 °C) and structurally (below 200 °C), together with the volatilization of the plasticizer and some compounds present in the algae [26]. In all cases it was observed that the mass loss in that temperature range (30–230 °C) by the samples with A was higher in comparison with the matrix, 75CH, which indicates that part of the algal biomass degrades at these temperatures [22, 53].

The position of the third degradation peak observed in all TGA curves increased with the content of A, suggesting an increase in thermal stability of the composites. A degrades over a wide range of temperatures with maximum degradation at 250, 278 and 346 °C, so an increase in the percentage of mass loss of that stage was observed since part of the algal biomass also degrades in that range of temperatures. As mentioned above, this type of algae has a high content of Alg and according to what was described by Soares et al. [53], this polymer degrades approximately 50% before 500 °C. The fourth stage of degradation represents a loss of mass close to 30% in all cases, except in the sample 75CH + 10A which presented an additional peak centered at 787.8 °C and representing a 15.8% loss of mass. This peak can be attributed to the formation of Na_2CO_3 as a residue of the thermal and oxidative degradation of Alg that begins at 500 °C and extends beyond 700 °C, according to Soares et al. [53] and/or to the presence of other inorganic salts [22]. Authors such as Jumaidin et al. [26] have also observed the appearance of a new peak of degradation at high temperatures and have attributed it to the decomposition of carbonates present in the alga [26].

Table 1 also incorporates the T_g values obtained from the DSC curves (see supplementary material) for TPS, CH, 75CH and their microcomposites with A. The TPS film presented a unique glass transition temperature close to − 78 °C, indicating good plasticization by glycerol [42]. The CH film, however, presented two transitions. Epure et al. [54], studied the CH-25% glycerol system by DMA and found two β-type relaxations and α-type relaxation, the latter being attributed to the T_g of the material (46 °C with 33% RH). B-relaxations were attributed to chain movements due to the presence of glycerol and water, respectively [54] and could be related here to the first observed transition. On the other hand, Bof et al. [55], who studied the effect of the molecular weight of CH in 50% mixtures with starch, found, when analyzing their samples by DMA, that CH films presented two relaxations, β and α, the first of them below -15 °C and the second between 30 and 80 °C, depending on the molecular weight of the CH analyzed. These authors attributed the transition below room temperature to local

movements of the lateral groups of the CH chain; while the second transition was associated with the glass transition temperature [55], these values being consistent with those found in this work.

In the 75CH sample, the plasticizing effect of the starch addition to a CH matrix was observed (higher proportion in the mixture) since the T_g runs towards lower temperatures [5]. In other words, if we consider that 25% of starch is incorporated into a CH matrix, a plasticizing effect is clearly observed in the latter. Chemically, the starch chains begin to interact with those of CH through the formation of hydrogen bonds, as previously seen by FTIR, reducing the number of CH–CH interactions and generating a more open structure, where the polymer chains have an greater mobility and therefore a lower T_g. Similar results were previously reported by other authors [55].

Regarding the microcomposites, in all cases, an inflection was observed in the curve below − 50 °C and in some cases, a second inflection was observed around 50 °C. The first one was related to the previously mentioned β relaxation and the second, relaxation α, with the T_g of the microcomposite. With the addition of A, a slight increase in the T_g of the 75CH matrix was observed, which suggests the presence of strong interactions by hydrogen bonds between the filler and the matrix, which restrict the molecular movements of the CH and the starch present in it [56, 57]. The absence of T_g in the microcomposites with 0.5 and 1% of A could be due to this same restriction in the molecular movement caused by the interaction with the filler [58]. Finally, a slight decrease in T_g by considerably increasing the content of A (10% A) could be due to the decrease in the number of interactions with the polymer given the formation of aggregates [56].

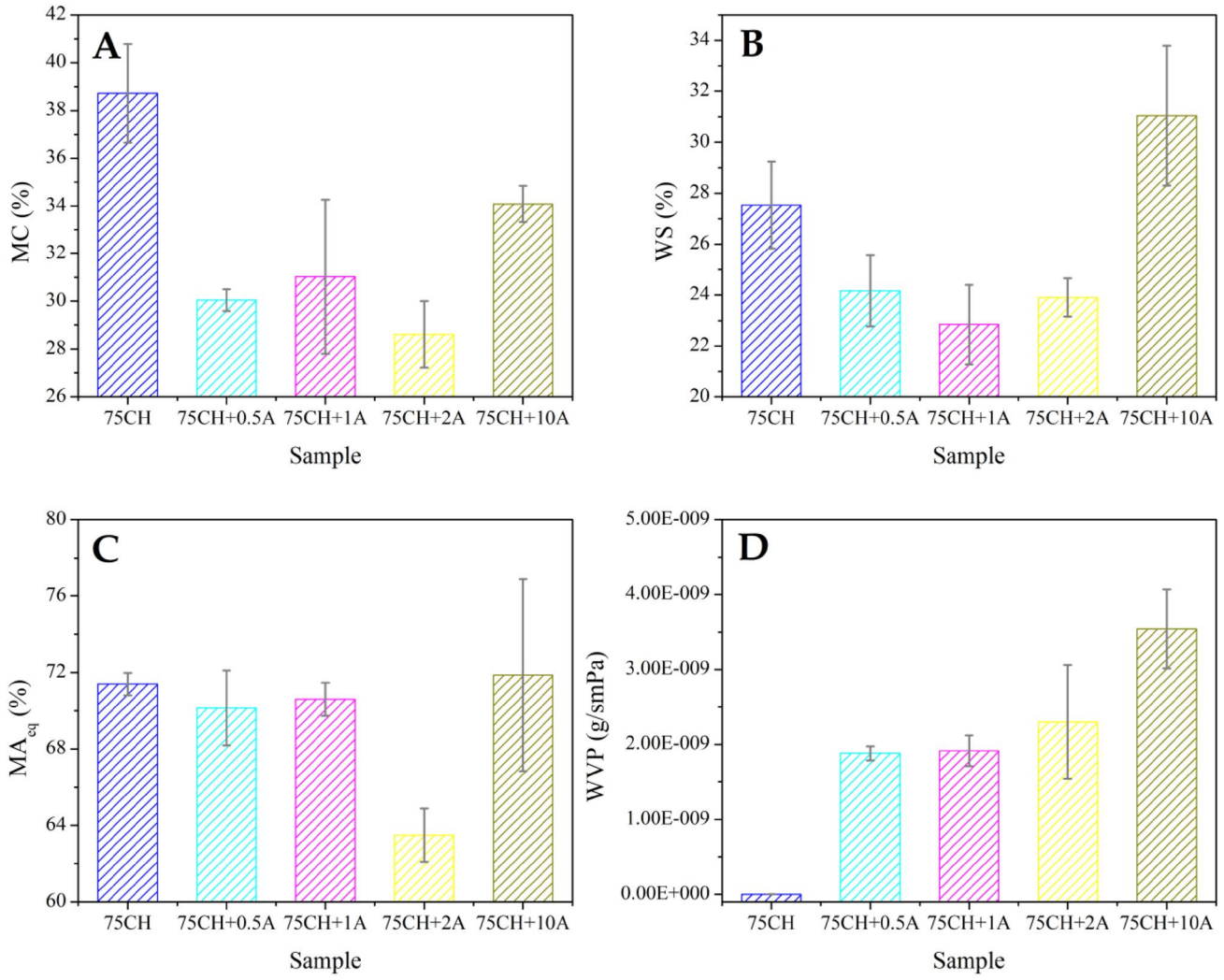

Fig. 5 Interaction of the microcomposites with water. **a** MC (%), **b** WS (%), **c** MA_{eq} (%) and **d** WVP (g/s m Pa) depending on the increasing content of **a** (%)

Figure 5 shows the results of the interaction of the materials with the water.

Figure 5a shows that microcomposites with low A content (0.5, 1 and 2%) had a lower MC than 75CH, while no significant differences were found between 75CH and 75CH + 10A. Similar results were previously reported by Jumaidin et al. [59] who found that the MC of starch/agar samples with aggregates of red algae showed a decrease of 1.5% in the MC from 0 to 40% of A. The authors explain that although the algae have a hydrophilic character, this may be reducing the mobility of the polymer chains, which would result in a lower MC [59]. The same tendencies were observed in the previously discussed DSC results.

The WS of the samples (Fig. 5b) was also not affected by the addition of A ($p < 0.05$), which suggests a good interaction between the components [59]. Jumaidin et al. [59] have reported an increase in WS of their microcomposites with higher aggregates of A justifying this result due to the swelling action of the algae that favors the disintegration of the polymer matrix [59].

It has been observed that the changes introduced in the structure by the addition of up to 10% of A have not produced significant differences in the MA_{eq} of the materials developed ($p < 0.05$), probably due to the fact that the incorporated contents of A are not sufficiently large enough to show an appreciable difference since these interact with the polymer matrix (Fig. 5c). Jumaidin et al. [59], worked with starch/agar micro-compounds and red seaweed of the species *Eucheuma cottonii* and reported a small difference in the MA for the sample with 10% of A and that this difference increased from 23.2 to 25.2% when going from 0 to 40% of A. These authors justify the observed behavior when considering the hydrophilic nature of the algae that facilitates the diffusion of water molecules in the material [59].

The contents of seaweed microparticles used in this work were notably lower than those of the mentioned work. However, it was clearly observed that the WVP increased with the content of A present (Fig. 5d). Although no significant differences were found between the samples with 0.5, 1 and 2% of A, it was found that, for the sample 75CH + 10%A, the permeability increased considerably. Increases in the WVP may be related to a lower association between molecules that facilitates the penetration of water molecules within the structure [59, 60], which is in accordance with the results obtained from the thermal characterization of the materials (TGA and DSC).

The microstructure of the films is determined by the spatial organization of the constituent polymer chains and by the way in which they interact. This analysis allows to obtain a better interpretation of the physical properties of the developed films [61]. Thus, the transverse surface of the microcomposites, obtained by fracture after immersion in liquid air, was studied by SEM. The obtained micrographs are shown in Fig. 6.

The 75CH mixture (Fig. 6a) presented a smooth and homogeneous fracture surface, which indicates that there is good compatibility between both polymers, as has been previously observed by other authors [61]. On the other hand, the alga used as filler presented a scaly morphology, with irregular edges and shapes of different sizes

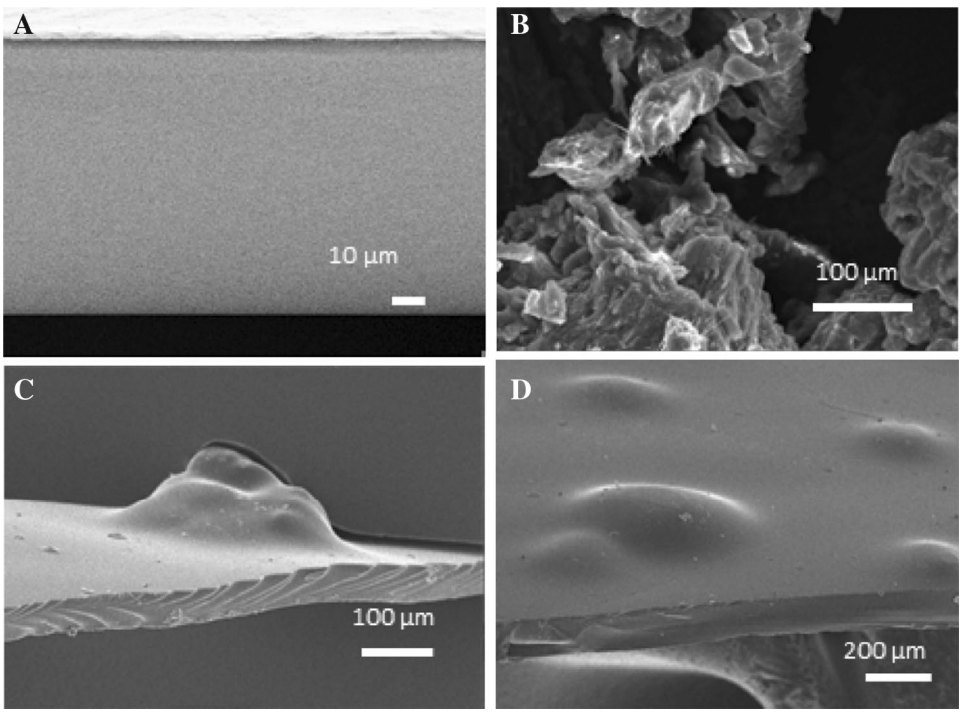

Fig. 6 SEM micrographs of **a** 75CH, **b** A, **c** 75CH + 0.5A and **d** 75CH + 10A

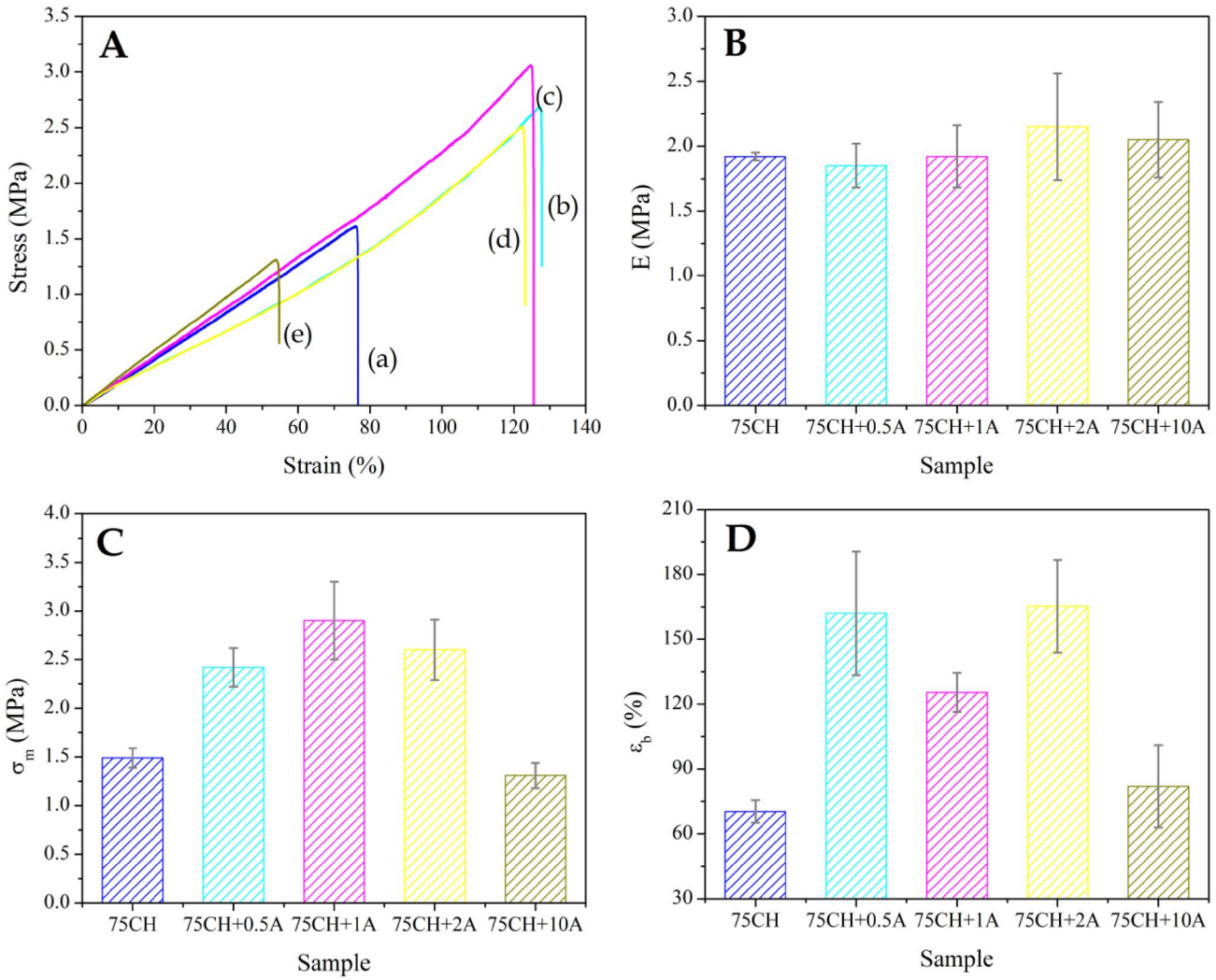

Fig. 7 Mechanical properties of the microcomposites according to the content of algae. **A** Stress (MPa) vs. strain (%) for *a* 75CH, *b* 75CH + 0.5A, *c* 75CH + 1A, *d* 75CH + 2A, *e* 75CH + 10A; **B** E (MPa), **C** σ_m (MPa) and **D** ε_b (%)

(Fig. 6b). Similar morphologies were previously described by Bulota and Budtova [22]. The micrograph obtained for 75CH + 0.5A (Fig. 6c), similar to those obtained with other contents of A, shows the presence of reliefs attributed to the presence of A particles of different sizes, with the highest observed of approximately 200 µm completely integrated in the polymer matrix. The cryofracture zone, on the other hand, presented a fragile fracture surface with striations.

The mechanical properties of 75CH and the effect produced by the addition of different contents of A are presented in Fig. 7.

It can be seen that E of all the microcomposites remained similar to that of 75CH, without showing significant differences between the different contents of A. In general, σ_m increased significantly for all microcomposites, although this increase was less significant with the increase in the percentage of incorporated algae, mainly for the sample 75CH + 10A, which suggests again that there is a good interaction between the filler and the matrix [52] and that at high contents of A discontinuities could appear [26]. Similar results were found for the formation of PVA/*Ulva armoricana* microcomposites [23] and starch/agar/*Eucheuma cottonii* [26]. The authors explain that these improvements in mechanical properties are due to the combination of materials that are chemically compatible, that is, there is a good adhesion of the polar A particles with the polar polymer matrix. On the contrary, when different species of algae were added in more hydrophobic matrices such as PLA, PCL, PHB and Mater-Bi, a decrease in the resistance of these materials has been reported [22, 62, 63].

The addition of low contents of A produced an increase in ε_b. However, no significant differences were observed between the materials 75CH + 0.5A, 1A and 2A. That is, A could be added up to 2% without altering the ε_b of that

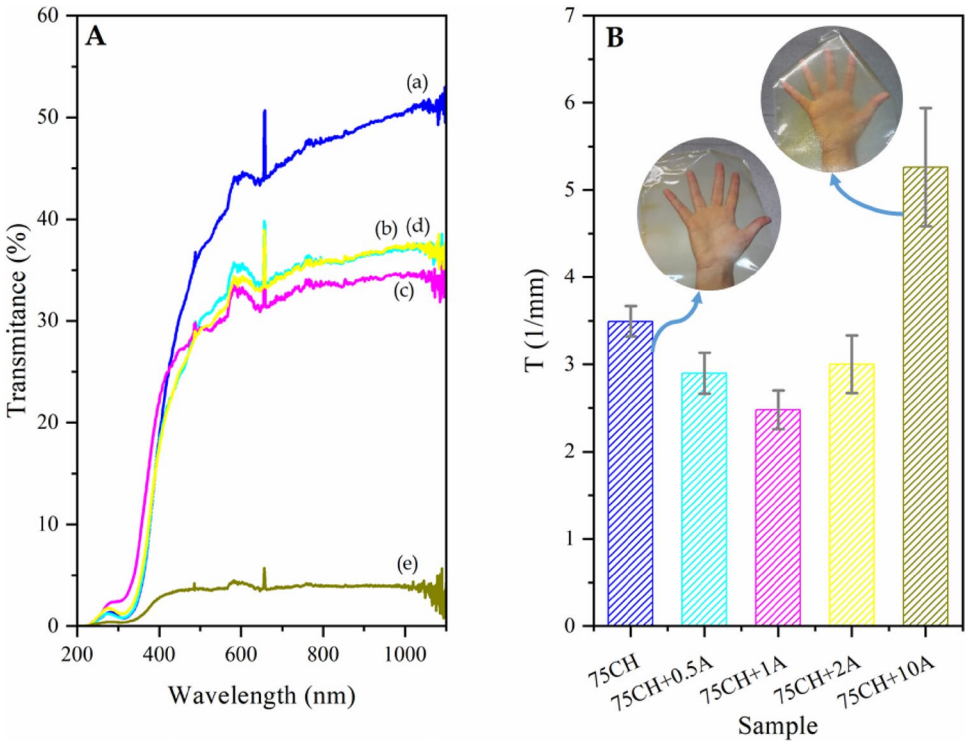

Fig. 8 Interaction of materials with light. **A** Transmittance spectra of UV–Vis radiation for *a* 75CH, *b* 75CH + 0.5A, *c* 75CH + 1A, *d* 75CH + 2A and *e* 75CH + 10A and, **B** T (1/mm)

materials. When the aggregate of A was 10% there was a significant decrease in the ε_b, which may be due to the presence of discontinuities caused by the agglomeration of these filler particles. When there are high contents of A, their particles act as discontinuities in the matrix and then produce a decrease in σ_m and ε_b [45] which is related with the observation on SEM images (Fig. 6).

Figure 8A shows the transmittance spectra of the UV–Vis radiation of the developed materials.

It was observed, in all cases, that it increases with the wavelength of the incident radiation, particularly from 400 nm, reaching a maximum of 50% transmittance for the 75CH sample. Compounds with A presented transmittance values lower than 40% in all cases. Figure 8B shows the results of T obtained when considering the thickness of the materials. These results suggest that the addition of amounts less than 2% of A produces more transparent films, probably due to the formation of a more open structure obtained as a consequence of the new interactions CH-A and TPS-A [61]. This hypothesis is in line with the results of Kadam et al. [64] or bovine gelatin films with algae extract *Ascophyllum nosodum*. Similar results were also reported by Bonilla et al. [9] for TPS-20%CH films with incorporation of different antioxidants as fillers. Subsequent increases in the content of A increase the opacity of the films. This behavior can be attributed to a greater dispersion of light due to the presence of a large number of particles of A, since these have dimensions much higher than those of the wavelength of the incident radiation [45, 65]. The results of the calculation of the coefficient of direct transmissivity of the materials in the PAR region are included in Table 1. It was found that sample 75CH presented the highest coefficient and that it decreased with the progressive increase in the A content.

Discussion

The results obtained from the characterization of TPS/CH + A microcomposites allow to carry out a discussion about the possible application of them in agriculture. In particular, the recent European norm EN 17033 provides information on the main requirements and test methods that biodegradable polymer films must meet to be applied as agricultural mulches. Among them, are the requirements for the mechanical and radiometric properties of these materials. The mechanical properties of the agricultural mulches must be sufficient to allow their mechanical placement maintaining their integrity to prevent ruptures. Therefore, it is proposed that they should have a σ_m in the direction of the machine direction (MD) and in the transverse direction (TD), greater than 16 MPa (MD) and 9 MPa (TD), while the ε_b, should be of 150% (MD) and 300% (TD). In addition, the radiometric properties are important because it can give us information about the effectiveness of the mulches to prevent the weeds growth. It is stated that the coefficient of direct transmissivity in the PAR region (wavelengths between 400 and 700 nm) must be under 3% [66]. A strategy to further reduce the

coefficient of transmissivity could include the addition of inorganic fillers, such as calcium carbonate or talc, which could allow obtaining opaque films that retain radiation of large wavelengths and prevent the growth of weeds [67, 68].

Although the developed materials have presented some improvements in mechanical properties with regard starch films, they were not enough to reach the requirements suggested for that application. However, its usefulness in other fields of research is not ruled out. For example, could be evaluated their use as wound dressing, edible films for food packaging or in cosmetics. The algae used in this work besides being exceptional for plants, have important dermatological and nutritional properties [69–71].

Conclusions

The effect of 75CH microcomposites by the addition of 0.5, 1, 2 and 10% of A was analyzed in terms of physicochemical, thermal, mechanical and morphological properties of films, and, their interaction with water and light. The used seaweed microparticles, rich in the Alg polymer, displayed good interactions with the 75CH matrix, produced an increase on the thermal stability of 75CH and an increase on the T_g of 75CH, indicating that the alga acts limiting the molecular movement of the polymer chains for its strong interaction. Incorporation of 10% of A could lead to a more heterogeneous structure with the formation of aggregates between alga particles. Low contents of A reduced the mobility of the polymer chains resulting in a lower MC and higher T_g. No changes were observed in the WS and the MA of the microcomposites, however, the WVP increased with the A content probably due to the formation of a more open structure. The presence of this structure could also be hypothesized thanks to the decrease in the transparency of the 75CH films with up to 2% of A. Regarding the mechanical properties, although no differences were found in the E of the different samples, it was possible to see that the addition of A produced an increase in the σ_m and a slight increase in the ε_b, which could indicates the formation of a structure that has a high interaction between its components and at the same time is more open, which allows the mobility of its chains. It is considered that the application of the developed materials in agricultural still need for further improvements while it is not discarded their utility in another fields of research.

Acknowledgements The authors acknowledge the National Research Council (CONICET), National Agency for Scientific and Technical Promotion (ANPCyT) and the National University of Mar del Plata (UNMdP) for the financial support and to the Dr. Diego Navarro, for the determination of starch molecular weight.

Compliance with Ethical Standards

Conflict of interest None.

References

1. Briassoulis D (2007) Analysis of the mechanical and degradation performances of optimised agricultural biodegradable films. Polym Degrad Stab 92:1115–1132. https://doi.org/10.1016/j.polymdegradstab.2007.01.024
2. Wortman SE, Kadoma I, Crandall MD (2015) Assessing the potential for spunbond, nonwoven biodegradable fabric as mulches for tomato and bell pepper crops. Sci Hortic (Amsterdam) 193:209–217. https://doi.org/10.1016/J.SCIENTA.2015.07.019
3. Pablo IA, Valiña A (2003) Cultivo bajo cubierta Zona sur de la provincia del Neuquén
4. Finkenstadt VL, Tisserat B (2010) Poly(lactic acid) and Osage orange wood fiber composites for agricultural mulch films. Ind Crops Prod 31:316–320. https://doi.org/10.1016/J.INDCROP.2009.11.012
5. Mitrus M (2010) TPS and its nature. Thermoplastic starch. Wiley-VCH Verlag GmbH & Co. KGaA, Weinheim, pp 77–104
6. Reis MO, Olivato JB, Bilck AP et al (2018) Biodegradable trays of thermoplastic starch/poly (lactic acid) coated with beeswax. Ind Crops Prod 112:481–487. https://doi.org/10.1016/J.INDCROP.2017.12.045
7. Carmona VB, Corrêa AC, Marconcini JM, Mattoso LHC (2015) Properties of a biodegradable ternary blend of thermoplastic starch (TPS), poly(ε-Caprolactone) (PCL) and poly(lactic acid) (PLA). J Polym Environ 23:83–89. https://doi.org/10.1007/s10924-014-0666-7
8. Akrami M, Ghasemi I, Azizi H et al (2016) A new approach in compatibilization of the poly(lactic acid)/thermoplastic starch (PLA/TPS) blends. Carbohydr Polym 144:254–262. https://doi.org/10.1016/J.CARBPOL.2016.02.035
9. Bonilla J, Talón E, Atarés L et al (2013) Effect of the incorporation of antioxidants on physicochemical and antioxidant properties of wheat starch–chitosan films. J Food Eng 118:271–278. https://doi.org/10.1016/J.JFOODENG.2013.04.008
10. Malerba M, Cerana R (2018) Recent advances of chitosan applications in plants. Polymers (Basel) 10:118. https://doi.org/10.3390/polym10020118
11. Xing K, Zhu X, Peng X, Qin S (2015) Chitosan antimicrobial and eliciting properties for pest control in agriculture: a review. Agron Sustain Dev 35:569–588. https://doi.org/10.1007/s13593-014-0252-3
12. Xoca-Orozco L-Á, Aguilera-Aguirre S, Vega-Arreguín J et al (2018) Activation of the phenylpropanoid biosynthesis pathway reveals a novel action mechanism of the elicitor effect of chitosan on avocado fruit epicarp. Food Res Int. https://doi.org/10.1016/J.FOODRES.2018.12.023
13. Singh A, Gairola K, Upadhyay V, Kumar J (2018) Chitosan: an elicitor and antimicrobial bio-resource in plant protection. Agric Rev 39:163–168
14. Merino D, Mansilla AY, Casalongué CA, Alvarez VA (2018) Preparation, characterization, and in vitro testing of nanoclay antimicrobial activities and elicitor capacity. J Agric Food Chem. https://doi.org/10.1021/acs.jafc.8b00049
15. Mansilla AY, Albertengo L, Rodríguez MS et al (2013) Evidence on antimicrobial properties and mode of action of a chitosan obtained from crustacean exoskeletons on *Pseudomonas syringae* pv. tomato DC3000. Appl Microbiol Biotechnol 97:6957–6966. https://doi.org/10.1007/s00253-013-4993-8

16. Terrile MC, Mansilla AY, Albertengo L et al (2015) Nitric-oxide-mediated cell death is triggered by chitosan in *Fusarium eumartii* spores. Pest Manag Sci 71:668–674. https://doi.org/10.1002/ps.3814
17. Pichyangkura R, Chadchawan S (2015) Biostimulant activity of chitosan in horticulture. Sci Hortic (Amsterdam) 196:49–65. https://doi.org/10.1016/j.scienta.2015.09.031
18. Rahman M, Mukta JA, Sabir AA et al (2018) Chitosan biopolymer promotes yield and stimulates accumulation of antioxidants in strawberry fruit. PLoS ONE 13:e0203769. https://doi.org/10.1371/journal.pone.0203769
19. Xu L, Geelen D (2018) Developing biostimulants from agro-food and industrial by-products. Front Plant Sci 9:1567. https://doi.org/10.3389/fpls.2018.01567
20. Battacharyya D, Babgohari MZ, Rathor P, Prithiviraj B (2015) Seaweed extracts as biostimulants in horticulture. Sci Hortic (Amsterdam) 196:39–48. https://doi.org/10.1016/J.SCIENTA.2015.09.012
21. Manivasagan P, Oh J (2016) Marine polysaccharide-based nanomaterials as a novel source of nanobiotechnological applications. Int J Biol Macromol 82:315–327. https://doi.org/10.1016/j.ijbiomac.2015.10.081
22. Bulota M, Budtova T (2015) PLA/algae composites: morphology and mechanical properties. Compos Part A Appl Sci Manuf 73:109–115. https://doi.org/10.1016/J.COMPOSITESA.2015.03.001
23. Chiellini E, Cinelli P, Ilieva VI, Martera M (2008) Biodegradable thermoplastic composites based on polyvinyl alcohol and algae. Biomacromolcules 9:1007–1013. https://doi.org/10.1021/bm701041e
24. Garrido T, Peñalba M, de la Caba K, Guerrero P (2016) Injection-manufactured biocomposites from extruded soy protein with algae waste as a filler. Compos Part B Eng 86:197–202. https://doi.org/10.1016/J.COMPOSITESB.2015.09.058
25. Torres S, Navia R, Campbell Murdy R et al (2015) Green composites from residual microalgae biomass and poly(butylene adipate-*co*-terephthalate): processing and plasticization. ACS Sustain Chem Eng 3:614–624. https://doi.org/10.1021/sc500753h
26. Jumaidin R, Sapuan SM, Jawaid M et al (2017) Effect of seaweed on mechanical, thermal, and biodegradation properties of thermoplastic sugar palm starch/agar composites. Int J Biol Macromol 99:265–273. https://doi.org/10.1016/j.ijbiomac.2017.02.092
27. Stawski D (2008) New determination method of amylose content in potato starch. Food Chem 110:777–781. https://doi.org/10.1016/j.foodchem.2008.03.009
28. De la Paz N, Pérez D, Fernández M et al (2013) Evaluación viscosimétrica del quitosano derivado de la quitina de langosta. Rev Iberoam Polímeros 14(2):84–91
29. Lavertu M, Xia Z, Serreqi AN et al (2003) A validated 1H NMR method for the determination of the degree of deacetylation of chitosan. J Pharm Biomed Anal 32:1149–1158. https://doi.org/10.1016/S0731-7085(03)00155-9
30. Balboa EM, Conde E, Moure A et al (2013) In vitro antioxidant properties of crude extracts and compounds from brown algae. Food Chem 138:1764–1785. https://doi.org/10.1016/J.FOODCHEM.2012.11.026
31. Britt K, Kangas P (2016) A preliminary assessment of dried algal biomass as a filler material in concrete. J Algal Biomass Util 7:147–152
32. American Society for Testing and Materials (2002) ASTM E96-00e1—Standard test methods for water vapor transmission of materials. ASTM, West Conshohocken, PA
33. Woggum T, Sirivongpaisal P, Wittaya T (2014) Properties and characteristics of dual-modified rice starch based biodegradable films. Int J Biol Macromol 67:490–502. https://doi.org/10.1016/J.IJBIOMAC.2014.03.029
34. ISO 9050:2003 (2003) Glass in building—determination of light transmittance, solar direct transmittance, total solar energy transmittance, ultraviolet transmittance and related glazing factors
35. Luchese CL, Pavoni JMF, dos Santos NZ et al (2018) Effect of chitosan addition on the properties of films prepared with corn and cassava starches. J Food Sci Technol 55:2963–2973. https://doi.org/10.1007/s13197-018-3214-y
36. Pelissari FM, Grossmann MVE, Yamashita F, Pineda EAG (2009) Antimicrobial, mechanical, and barrier properties of cassava starch–chitosan films incorporated with oregano essential oil. J Agric Food Chem 57:7499–7504. https://doi.org/10.1021/jf902363
37. Bourtoom T (2008) Plasticizer effect on the properties of biodegradable blend film from rice starch-chitosan. Songklanakarin J Sci Technol 30:149–155
38. Ren L, Yan X, Zhou J et al (2017) Influence of chitosan concentration on mechanical and barrier properties of corn starch/chitosan films. Int J Biol Macromol 105:1636–1643. https://doi.org/10.1016/j.ijbiomac.2017.02.008
39. Mei J, Yuan Y, Wu Y, Li Y (2013) Characterization of edible starch–chitosan film and its application in the storage of Mongolian cheese. Int J Biol Macromol 57:17–21. https://doi.org/10.1016/J.IJBIOMAC.2013.03.003
40. Bourtoom T, Chinnan MS (2008) Preparation and properties of rice starch–chitosan blend biodegradable film. LWT Food Sci Technol 41:1633–1641. https://doi.org/10.1016/J.LWT.2007.10.014
41. Mollah MZI, Akter N, Quader FB et al (2016) Biodegradable colour polymeric film (starch-chitosan) development: characterization for packaging materials. Open J Org Polym Mater 06:11–24. https://doi.org/10.4236/ojopm.2016.61002
42. Mathew S, Brahmakumar M, Abraham TE (2006) Microstructural imaging and characterization of the mechanical, chemical, thermal, and swelling properties of starch–chitosan blend films. Biopolymers 82:176–187. https://doi.org/10.1002/bip.20480
43. Zhong Y, Song X, Li Y (2011) Antimicrobial, physical and mechanical properties of kudzu starch–chitosan composite films as a function of acid solvent types. Carbohydr Polym 84:335–342. https://doi.org/10.1016/J.CARBPOL.2010.11.041
44. Dang KM, Yoksan R (2016) Morphological characteristics and barrier properties of thermoplastic starch/chitosan blown film. Carbohydr Polym 150:40–47. https://doi.org/10.1016/J.CARBPOL.2016.04.113
45. Valencia-Sullca C, Vargas M, Atarés L, Chiralt A (2018) Thermoplastic cassava starch-chitosan bilayer films containing essential oils. Food Hydrocoll 75:107–115. https://doi.org/10.1016/J.FOODHYD.2017.09.008
46. Lozano-Navarro J, Díaz-Zavala N, Velasco-Santos C et al (2018) Chitosan-starch films with natural extracts: physical, chemical, morphological and thermal properties. Materials (Basel) 11:120. https://doi.org/10.3390/ma11010120
47. Gómez-Ordóñez E, Rupérez P (2011) FTIR-ATR spectroscopy as a tool for polysaccharide identification in edible brown and red seaweeds. Food Hydrocoll 25:1514–1520. https://doi.org/10.1016/J.FOODHYD.2011.02.009
48. Merino D, Gutierrez T, Alvarez VA (2019) Potential agricultural mulch films based on native and phosphorylated corn starch with and without surface functionalization with chitosan. J Polym Environ 27:97–105
49. Debandi MV, Bernal C, Francois NJ (2016) Development of biodegradable films based on chitosan/glycerol blends suitable for biomedical applications. J Tissue Sci Eng 7:1–9
50. Aouada FA, Mattoso LHC, Longo E (2011) New strategies in the preparation of exfoliated thermoplastic starch–montmorillonite nanocomposites. Ind Crops Prod 34:1502–1508. https://doi.org/10.1016/j.indcrop.2011.05.003

51. Mendes JF, Paschoalin R, Carmona VB et al (2016) Biodegradable polymer blends based on corn starch and thermoplastic chitosan processed by extrusion. Carbohydr Polym 137:452–458. https://doi.org/10.1016/J.CARBPOL.2015.10.093
52. Yan C, Wang R, Wan J et al (2016) Cellulose/microalgae composite films prepared in ionic liquids. Algal Res 20:135–141. https://doi.org/10.1016/J.ALGAL.2016.09.024
53. Soares JP, Santos JE, Chierice GO, Cavalheiro ETG (2004) Thermal behavior of alginic acid and its sodium salt. Eclética Química 29:57–64. https://doi.org/10.1590/S0100-46702004000200009
54. Epure V, Griffon M, Pollet E, Avérous L (2011) Structure and properties of glycerol-plasticized chitosan obtained by mechanical kneading. Carbohydr Polym 83:947–952. https://doi.org/10.1016/J.CARBPOL.2010.09.003
55. Bof MJ, Bordagaray VC, Locaso DE, García MA (2015) Chitosan molecular weight effect on starch-composite film properties. Food Hydrocoll 51:281–294. https://doi.org/10.1016/J.FOODHYD.2015.05.018
56. Li Q, Zhou J, Zhang L (2009) Structure and properties of the nanocomposite films of chitosan reinforced with cellulose whiskers. J Polym Sci Part B Polym Phys 47:1069–1077. https://doi.org/10.1002/polb.21711
57. Chen L, Tang C, Ning N et al (2009) Preparation and properties of chitosan/lignin composite films. Chin J Polym Sci 27:739. https://doi.org/10.1142/S0256767909004448
58. Niazi MBK, Broekhuis AA (2015) Surface photo-crosslinking of plasticized thermoplastic starch films. Eur Polym J 64:229–243. https://doi.org/10.1016/j.eurpolymj.2015.01.027
59. Jumaidin R, Sapuan SM, Jawaid M et al (2016) Effect of seaweed on physical properties of thermoplastic sugar palm starch/agar composites. J Mech Eng Sci 10:2214–2225. https://doi.org/10.15282/jmes.10.3.2016.1.0207
60. Escamilla-García M, Reyes-Basurto A, García-Almendárez B et al (2017) Modified starch-chitosan edible films: physicochemical and mechanical characterization. Coatings 7:224. https://doi.org/10.3390/coatings7120224
61. Talón E, Trifkovic KT, Nedovic VA et al (2017) Antioxidant edible films based on chitosan and starch containing polyphenols from thyme extracts. Carbohydr Polym 157:1153–1161. https://doi.org/10.1016/J.CARBPOL.2016.10.080
62. Barghini A, Ivanova VI, Imam SH, Chiellini E (2010) Poly-(ε-caprolactone) (PCL) and poly(hydroxy-butyrate) (PHB) blends containing seaweed fibers: morphology and thermal-mechanical properties. J Polym Sci Part A Polym Chem 48:5282–5288. https://doi.org/10.1002/pola.24327
63. Iannace S, Nocilla G, Nicolais L (1999) Biocomposites based on sea algae fibers and biodegradable thermoplastic matrices. J Appl Polym Sci 73:583–592. https://doi.org/10.1002/(SICI)1097-4628(19990725)73:4%3c583:AID-APP14%3e3.0.CO;2-H
64. Kadam SU, Pankaj SK, Tiwari BK et al (2015) Development of biopolymer-based gelatin and casein films incorporating brown seaweed *Ascophyllum nodosum* extract. Food Packag Shelf Life 6:68–74. https://doi.org/10.1016/J.FPSL.2015.09.003
65. Rhim J-W (2011) Effect of clay contents on mechanical and water vapor barrier properties of agar-based nanocomposite films. Carbohydr Polym 86:691–699. https://doi.org/10.1016/J.CARBPOL.2011.05.010
66. Sartore L, Vox G, Schettini E (2013) Preparation and performance of novel biodegradable polymeric materials based on hydrolyzed proteins for agricultural application. J Polym Environ 21:718–725. https://doi.org/10.1007/s10924-013-0574-2
67. Robinson D, Brae B (1991) Developments in plastic structures and materials for horticultural crops. ASPAC, Food Fertil Technol Center
68. Vox G, Santagata G, Malinconico M et al (2013) Biodegradable films and spray coatings as eco-friendly alternative to petro-chemical derived mulching films. J Agric Eng. https://doi.org/10.4081/jae.2013.286
69. Wang HMD, Chen CC, Huynh P, Chang JS (2015) Exploring the potential of using algae in cosmetics. Bioresour Technol 184:355–362. https://doi.org/10.1016/j.biortech.2014.12.001
70. Sathasivam R, Radhakrishnan R, Hashem A, Abd_Allah EF (2017) Microalgae metabolites: a rich source for food and medicine. Saudi J Biol Sci 26:709–722. https://doi.org/10.1016/j.sjbs.2017.11.003
71. Venkatesan J, Lowe B, Anil S et al (2015) Seaweed polysaccharides and their potential biomedical applications. Starch/Staerke 67:381–390. https://doi.org/10.1002/star.201400127